Acta Cryst E CRYSTALLOGRAPHIC COMMUNICATIONS

ISSN 2056-9890

Crystal structure and Hirshfeld surface analysis of *N*-(1*H*-benzo[*d*]imidazol-2-yl)acetamide

Akmaljon G. Tojiboev,[a]*‡ Rasul Okmanov,[b] Asqar Abdurazakov,[b] Sarvar Saidov,[b] Elyor Rakhmatov,[b] Abduakhad Kodirov[c] and Burkhon Elmuradov[b]

[a]University of Geological Sciences, Olimlar str. 64, Tashkent 100170, Uzbekistan, [b]Institute of the Chemistry of Plant Substances, Uzbekistan Academy of Sciences, Mirzo Ulugbek Str. 77, Tashkent 100170, Uzbekistan, and [c]Karshi State University, Kuchabog str. 17, Karshi 180119, Uzbekistan. *Correspondence e-mail: a_tojiboev@yahoo.com

Received 17 March 2026
Accepted 21 April 2026

Edited by M. Weil, Vienna University of Technology, Austria

‡ Branch of the Russian Chemical-Technological University named after D.I. Mendeleev in Tashkent Uzbekistan

Keywords: hydrogen bonding; crystal structure; Hirshfeld surface analysis; benzimidazole.

CCDC reference: 2394740

Supporting information: this article has supporting information at journals.iucr.org/e

The crystal structure of the title compound, $C_9H_9N_3O$, was refined using non-spherical scattering factors. This quantum crystallographic approach provided enhanced precision for the H-atom positions and a refined description of the electron density. The asymmetric unit comprises two molecules (Z' = 2) exhibiting high conformational similarity (r.m.s. deviation between the molecules is 0.083 Å). In the crystal, molecules form pseudocentrosymmetric dimers *via* intermolecular N—H···O and N—H···N hydrogen bonds. These units are further linked into supramolecular layers characterized by $D(1)$, $C_2^2(8)$, $C_2^2(10)$, $R_2^2(8)$ and $R_2^2(12)$ graph-set motifs. The packing is mainly consolidated by C—H···π interactions. Hirshfeld surface analysis and two-dimensional fingerprint plots were used to quantify the supramolecular assembly, identifying H···H (45%), C···H/H···C (20.8%), N···H/H···N (12.2%) and O···H/H···O (11.5%) contacts as the primary contributors to the crystal packing.

1. Chemical context

Benzimidazole is a bicyclic heteroaromatic organic compound consisting of a benzene ring and an imidazole ring, which enables chemists to carry out targeted electrophilic and nucleophilic substitution or addition reactions (Faheem *et al.*, 2020). Substituted benzimidazoles constitute an important class of heterocyclic compounds that are of interest to both theoretical organic chemists and representatives of the pharmaceutical industry (Lee *et al.*, 2023), in particular due to their antimicrobial, anthelmintic, antiviral and anticancer activities, or their use as antihypertensives and antihistamines, *e.g.* astemizole or bilastine (Chung *et al.*, 2023).

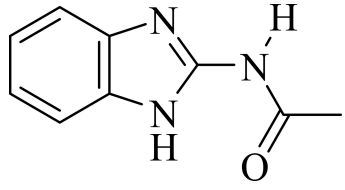

In this context, we report the synthesis and crystal structure determination of *N*-(1*H*-benzo[*d*]imidazol-2-yl)acetamide, (**1**), and provide the results of a Hirshfeld surface analysis.

2. Structural commentary

The asymmetric unit of compound (**1**) comprises two molecules designated as *A* and *B* (Fig. 1). Molecules *A* and *B* form a pseudocentrosymmetric dimer consolidated by two non-equivalent intermolecular N1*A*—H1*A*···O1*B* and N1*B*—

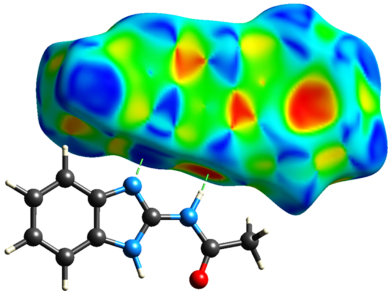

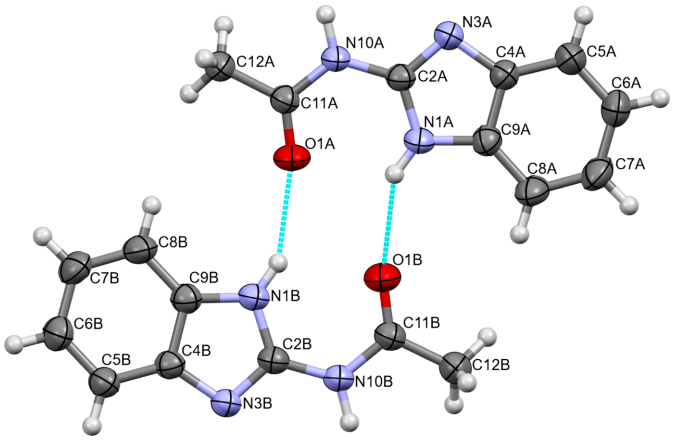

Figure 1
The structures of independent molecules *A* and *B* in compound (**1**), with the atom-labeling scheme and displacement ellipsoids drawn at the 50% probability level (H atoms are shown as spheres of arbitrary size). Intermolecular N1*A*—H1*A*···O1*B* and N1*B*—H1*B*···O1*A* hydrogen bonds are shown as blue dashed lines.

H1*B*···O1*A* hydrogen bonds (Table 1; entries 1 and 2). In each case, the molecular structure is stabilized by an intramolecular N—H···O hydrogen bond (Table 1; entries 3 and 4), which leads to the formation of a five-membered ring. The r.m.s. deviation between the non-H atoms of molecules *A* and *B* is 0.083 Å, indicating a high degree of structural similarity (Fig. 2). Both molecules are essentially planar, with r.m.s. deviations of 0.0123 (for *A*) and 0.0122 Å (for *B*). The planarity is further supported by torsion angles C11—N10—C2—N3 = 170.41 (11)° for *A* and −175.67 (12)° for *B*, which deviate only slightly from the ideal antiperiplanar value of 180°. The observed planarity facilitates maximum π-electron conjugation and *p*-orbital overlap, providing the molecular framework with substantial electronic stability.

3. Supramolecular features

In the crystal, the interplay between intra- and intermolecular N—H···O hydrogen bonds (Table 1, entries 1–4), as well as of intermolecular N—H···N hydrogen bonds (Table 1; entries 5 and 6), leads to the formation of chains propagating parallel to the *b* axis (Fig. 3) and gives rise to $D(1)$, $C_2^2(8)$, $C_2^2(10)$, $R_2^2(8)$ and $R_2^2(12)$ graph-set motifs (Etter *et al.*, 1990). The molecules in adjacent chains interact mainly through C—H···π interactions, specifically C12*A*—H12*B*···*Cg*2 [3.523 (2) Å], C12*B*—H12*E*···*Cg*4 [3.526 (2) Å] and C12*B*—H12*F*···*Cg*5 [3.526 (2) Å] [*Cg*2 is the centroid of ring C4*A*–C9*A*, *Cg*4 is the centroid of ring N1*B*/C2*B*/N3*B*/C4*B*/C9*B* and *Cg*5 is the centroid of ring C4*B*–C9*B*] (Fig. S1 in the supporting information). These interactions contribute to a herringbone packing motif in the crystal structure (Fig. S2).

Table 1
Hydrogen-bond geometry (Å, °).

D—H···*A*	*D*—H	H···*A*	*D*···*A*	*D*—H···*A*
N1*A*—H1*A*···O1*B*	1.03 (1)	2.06 (1)	2.9647 (15)	145 (1)
N1*B*—H1*B*···O1*A*	1.03 (1)	2.05 (1)	2.9693 (15)	148 (1)
N1*A*—H1*A*···O1*A*	1.03 (1)	2.10 (1)	2.6780 (16)	114 (1)
N1*B*—H1*B*···O1*B*	1.03 (1)	2.10 (1)	2.6822 (17)	114 (1)
N10*A*—H10*A*···N3*B*^{i}	1.031 (15)	1.948 (15)	2.9757 (16)	174.7 (13)
N10*B*—H10*B*···N3*A*^{ii}	1.026 (14)	1.962 (14)	2.9837 (16)	173.7 (11)

Symmetry codes: (i) $x, y+1, z$; (ii) $x, y-1, z$.

4. Database survey

A search of the Cambridge Structural Database (CSD, Version 2025.3.0; Groom *et al.*, 2016) for structures containing the 2-acetamidobenzimidazole moiety with similar planarity yielded ten relevant hits. These include refcodes BELYEA (Bhardwaj *et al.*, 2022), FIZSUF (Odame *et al.*, 2018), LUMCAA (Gergely *et al.*, 2020), PUPJIW (Al-Taie *et al.*, 2020), PUPJOC (Al-Taie *et al.*, 2020), PUPJUI (Al-Taie *et al.*, 2020), SOVZAH (Srinivasarao *et al.*, 2019), VADKIY (Singh *et al.*, 2017), WEDJIC (Kumari *et al.*, 2022) and XENKAD (Yang *et al.*, 2006). As already noted, compound (**1**) exhibits a high degree of planarity, which is a common feature among the surveyed structures. However, significant differences arise in the orientation of the acetamide substituent. The conformation is primarily governed by the C11—N10—C2—N3 torsion angle. Molecule *A* of the title compound shows a nearly coplanar arrangement, closely resembling the conformations found in LUMCAA and XENKAD. In contrast, molecule *B* exhibits a slight twist that correlates more closely with the molecular shape of FIZSUF. Furthermore, the CSD survey reveals two competing hydrogen-bonding motifs for this class of compounds. While many derivatives, such as PUPJIW and SOVZAH, favour the formation of centrosymmetric $R_2^2(8)$ dimers, the title compound utilizes both molecules *A* and *B* to establish a pseudocentrosymmetric dimer through N—H···O interactions. This specific assembly is influenced by the steric requirements of the benzimidazole core, distinguishing it from

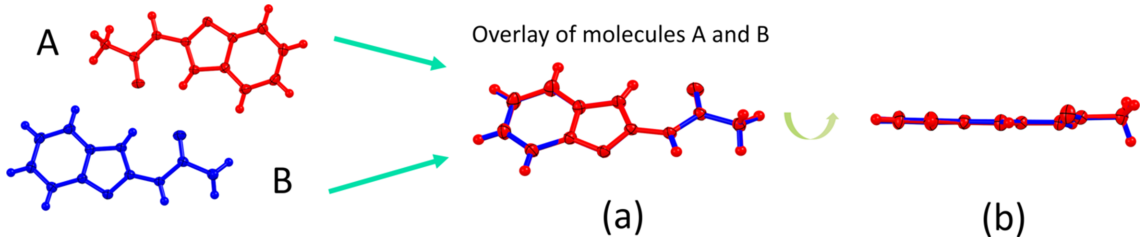

Figure 2
(*a*) Superposition of molecule *A* (red) and molecule *B* (blue) in the title compound, and (*b*) side views of molecules *A* and *B* to show their planarity.

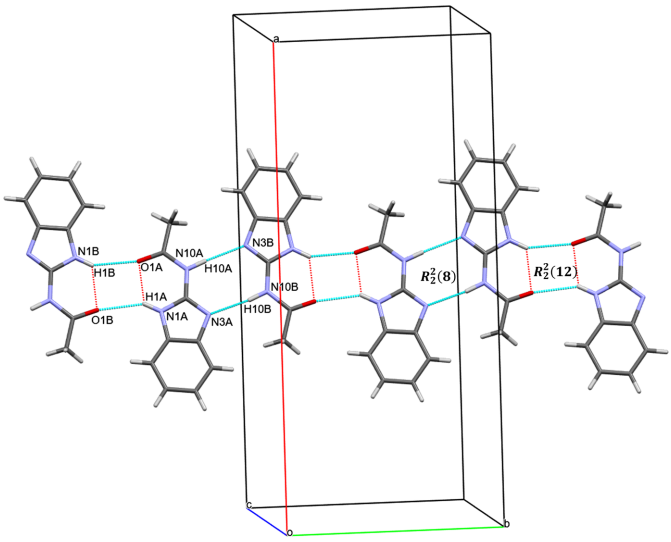

Figure 3
Intramolecular N1*B*—H1*B*···O1*B* hydrogen bonds (red dashed lines) and intermolecular N1*B*—H1*B*···O1*A*, N1*A*—H1*A*···O1*B*, N10*A*—H10*A*···N3*B*, N10*B*—H10*B*···N3*A* hydrogen bonds (blue dashed lines). The $R_2^2(8)$ and $R_2^2(12)$ graph-set motifs, extending parallel to the *b* axis, are generated by a combination of N—H···N and N—H···O hydrogen bonds.

the simpler chain motifs as observed, for example, in VADKIY.

5. Hirshfeld surface analysis

To gain deeper insight into the intermolecular interactions within the title compound, a Hirshfeld surface (HS) analysis was carried out, and two-dimensional fingerprint plots were generated using *CrystalExplorer* (Spackman *et al.*, 2021). The HS mapped over d_{norm}, and the shape index as a visual representation of the contacts, are shown in Fig. 4. The d_{norm} surface exhibits prominent deep-red spots, which correspond to the closest contact distances, specifically representing the donor and acceptor sites of the intermolecular N—H···O and N—H···N hydrogen bonds. The relative contributions of the various intermolecular contacts were quantified using two-

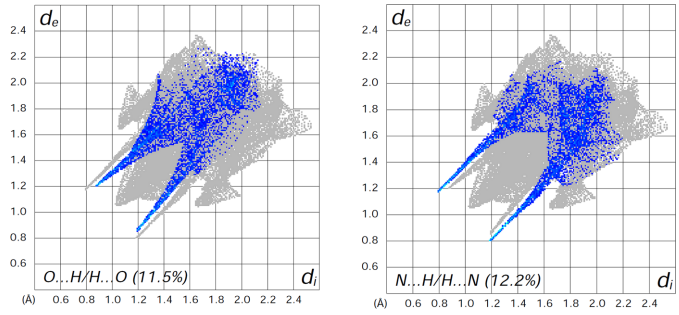

Figure 5
Two-dimensional fingerprint plots for the title compound, decomposed into (left) O···H/H···O (11.5%) and (right) N···H/H···N (12.2%) contacts.

dimensional fingerprint plots (Fig. S3 in the supporting information), revealing that the stability of the crystal packing is primarily governed by H···H contacts, which constitute the largest contribution at 45.0%. The significant role of C—H···π interactions is evidenced by the C···H/H···C contacts (20.8%). The presence of classical hydrogen bonding is clearly manifested as a pair of characteristic sharp 'spikes' in the fingerprint plots (Fig. 5) for N—H···N interactions (represented by N···H/H···N contacts, 12.2%) and N—H···O amide interactions (represented by O···H/H···O contacts, 11.5%). A detailed inspection of the shape index map reveals a pattern of red and blue triangles ('bow-tie' patterns) and complementary flat regions on the curvedness map. These features, combined with the C···C contribution (2.0%), are indicative of weak π–π stacking interactions between the benzimidazole rings. Minor contributions from C···O/O···C (3.1%), N···C/C···N (2.2%) and other contacts (totaling approximately 3.2%) further facilitate the supramolecular assembly in the crystal.

6. Synthesis and crystallization

The reaction of methylbenzimidazol-2-yl carbamate with glacial acetic acid was carried out at the boiling point of the acid for 8 h. As a result of the reaction, *N*-(1*H*-benzimidazol-2-yl)acetamide was synthesized (Fig. 6) in almost quantitative

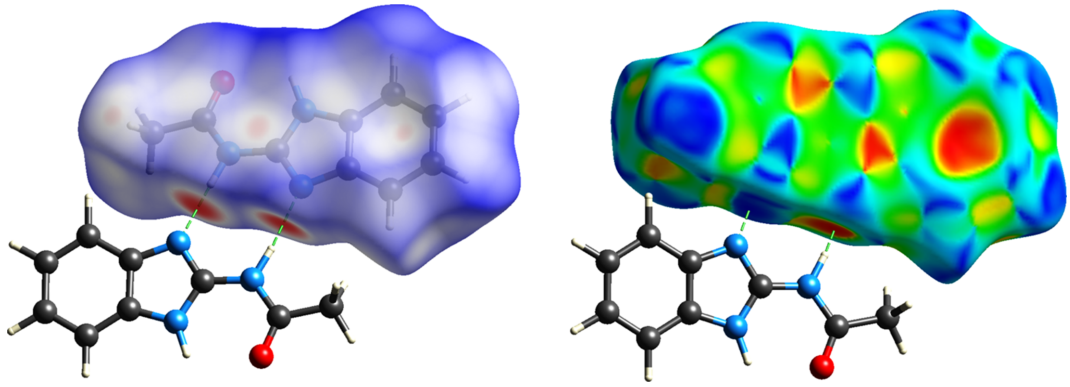

Figure 4
Hirshfeld surface of (**1**), mapped over d_{norm} (left) and shape index (right), showing close intermolecular contacts.

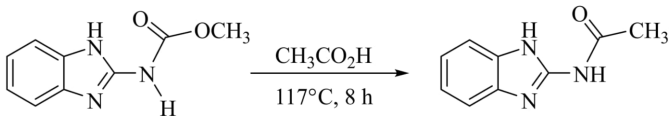

Figure 6
Synthesis scheme to obtain the title compound.

yield (Abdurazakov *et al.*, 2021). Colourless single crystals suitable for X-ray diffraction analysis were obtained by recrystallization from methanol.

7. Refinement

Crystal data, data collection and structure refinement details are summarized in Table 2. H atoms were first positioned geometrically [aromatic C—H = 0.93 Å and N—H = 0.86 Å, and in the acetamido fragment N—H = 0.924 (16) Å] and refined using a riding model, with U_{iso}(H) = 1.2U_{eq}(aromatic C, N) or 1.5U_{eq}(methyl C). The structure was finally refined using the *NoSpherA2* (Kleemiss *et al.*, 2021) implementation within *OLEX2* (Bourhis *et al.*, 2015). Non-spherical atomic scattering factors were calculated using the *ORCA* (Neese, 2012) software package at the r2SCAN/3-21G (Furness *et al.*, 2020) level of theory. The RIJCOSX approximation with the def2/J auxiliary basis set was employed to accelerate the calculation of the electronic structure. This approach allowed for a more accurate treatment of the electron density, particularly for H-atom positions and the resulting intermolecular interactions.

Table 2
Experimental details.

Crystal data	
Chemical formula	$C_9H_9N_3O$
M_r	175.19
Crystal system, space group	Orthorhombic, *Pbcn*
Temperature (K)	293
a, *b*, *c* (Å)	23.011 (5), 10.167 (2), 14.294 (3)
V (Å^3)	3344.0 (12)
Z	16
Radiation type	Cu *Kα*
μ (mm^{-1})	0.79
Crystal size (mm)	0.30 × 0.25 × 0.25
Data collection	
Diffractometer	XtaLAB Synergy, Single source at home/near, HyPix3000
Absorption correction	Multi-scan (*CrysAlis PRO*; Rigaku OD, 2020)
T_{min}, T_{max}	0.906, 1.000
No. of measured, independent and observed [$I \geq 2u(I)$] reflections	32896, 3484, 2875
R_{int}	0.050
(sin $\theta/\lambda)_{max}$ (Å^{-1})	0.629
Refinement	
$R[F^2 > 2\sigma(F^2)]$, $wR(F^2)$, *S*	0.035, 0.103, 1.05
No. of reflections	3484
No. of parameters	246
H-atom treatment	H atoms treated by a mixture of independent and constrained refinement
$\Delta\rho_{max}$, $\Delta\rho_{min}$ (e Å^{-3})	0.23, −0.25

Computer programs: *CrysAlis PRO* (Rigaku OD, 2020), *SHELXT* (Sheldrick, 2015), *OLEX2*.refine (Bourhis *et al.*, 2015), *OLEX2* (Dolomanov *et al.*, 2009) and *publCIF* (Westrip, 2010).

Acknowledgements

This work was supported by the Academy of Sciences of the Republic of Uzbekistan, and the CCDC FAIRE programme provided access to the CSD and its software suite.

References

Abdurazakov, A. Sh., Saidov, S. S., Okmanov, R. Ya., Kubaev, Sh. Kh. & Elmuradov, B. Zh. (2021). *Egypt. J. Chem.* **64**, 2247–2252.
Al-Taie, Z. S., Anetts, S. R., Christensen, J., Coles, S. J., Horton, P. N., Evans, D. M., Jones, L. F., de Kleijne, F. F. J., Ledbetter, S. M., Mehdar, Y. T. H., Murphy, P. J. & Wilson, J. A. (2020). *RSC Adv.* **10**, 22397–22416.
Bhardwaj, V., Salunke, P. S., Puranik, A. A., Kulkarni, N. D. & Ballabh, A. (2022). *Polyhedron* **225**, 116054.
Bourhis, L. J., Dolomanov, O. V., Gildea, R. J., Howard, J. A. K. & Puschmann, H. (2015). *Acta Cryst.* A**71**, 59–75.
Chung, N. T., Dung, V. C. & Duc, D. X. (2023). *RSC Adv.* **13**, 32734–32771.
Dolomanov, O. V., Bourhis, L. J., Gildea, R. J., Howard, J. A. K. & Puschmann, H. (2009). *J. Appl. Cryst.* **42**, 339–341.
Etter, M. C., MacDonald, J. C. & Bernstein, J. (1990). *Acta Cryst.* B**46**, 256–262.
Faheem, M., Rathaur, A., Pandey, A., Singh, V. K. & Tiwari, A. K. (2020). *ChemistrySelect* **5**, 3981–3994.
Furness, J. W., Kaplan, A. D., Ning, J., Perdew, J. P. & Sun, J. (2020). *J. Phys. Chem. Lett.* **11**, 8208–8215.
Gergely, M., Bényei, A. & Kollár, L. (2020). *Tetrahedron* **76**, 131079.
Groom, C. R., Bruno, I. J., Lightfoot, M. P. & Ward, S. C. (2016). *Acta Cryst.* B**72**, 171–179.
Kleemiss, F., Dolomanov, O. V., Bodensteiner, M., Peyerimhoff, N., Midgley, L., Bourhis, L. J., Genoni, A., Malaspina, L. A., Jayatilaka, D., Spencer, J. L., White, F., Grundkötter-Stock, B., Steinhauer, S., Lentz, D., Puschmann, H. & Grabowsky, S. (2021). *Chem. Sci.* **12**, 1675–1692.
Kumari, A., Dehaen, W., Chopra, D. & Dey, S. (2022). *New J. Chem.* **46**, 10628–10636.
Lee, Y. T., Tan, Y. J. & Oon, Ch. E. (2023). *Acta Pharm. Sin. B* **13**(2), 478-497.
Neese, F. (2012). *WIREs Comput. Mol. Sci.* **2**, 73–78.
Odame, F., Betz, R., Hosten, E. C., Krause, J., Isaacs, M., Hoppe, H. C., Khanye, S. D., Sayed, Y., Frost, P. C., Lobb, K. A. & Tshentu, Z. R. (2018). *ChemistrySelect* **3**, 13613–13618.
Rigaku OD (2020). *CrysAlis PRO*. Rigaku Oxford Diffraction Ltd, Yarnton, Oxfordshire, England.
Sheldrick, G. M. (2015). *Acta Cryst.* C**71**, 3–8.
Singh, V., Kant, R. & Agarwal, A. (2017). *Proc. Natl Acad. Sci. India, Sect. A Phys. Sci.* **87**, 321–331.
Spackman, P. R., Turner, M. J., McKinnon, J. J., Wolff, S. K., Grimwood, D. J., Jayatilaka, D. & Spackman, M. A. (2021). *J. Appl. Cryst.* **54**, 1006–1011.
Srinivasarao, S., Nandikolla, A., Nizalapur, S., Yu, T. T., Pulya, S., Ghosh, B., Murugesan, S., Kumar, N. & Chandra Sekhar, K. V. G. (2019). *RSC Adv.* **9**, 29273–29292.
Westrip, S. P. (2010). *J. Appl. Cryst.* **43**, 920–925.
Yang, B., Xia, Y.-F., Bi, S. & Zhang, S.-S. (2006). *Acta Cryst.* E**62**, o4200–o4202.

supporting information

Acta Cryst. (2026). E**82**, 521-524 [https://doi.org/10.1107/S2056989026004196]

Crystal structure and Hirshfeld surface analysis of *N*-(1*H*-benzo[*d*]imidazol-2-yl)acetamide

Akmaljon G. Tojiboev, Rasul Okmanov, Asqar Abdurazakov, Sarvar Saidov, Elyor Rakhmatov, Abduakhad Kodirov and Burkhon Elmuradov

Computing details

N-(1*H*-Benzo[*d*]imidazol-2-yl)acetamide

Crystal data

$C_9H_9N_3O$
M_r = 175.19
Orthorhombic, *Pbcn*
a = 23.011 (5) Å
b = 10.167 (2) Å
c = 14.294 (3) Å
V = 3344.0 (12) Å^3
Z = 16
F(000) = 1477.168
D_x = 1.392 Mg m^{-3}
Cu *Kα* radiation, *λ* = 1.54184 Å
Cell parameters from 9360 reflections
θ = 4.3–75.7°
μ = 0.79 mm^{-1}
T = 293 K
Prism, colourless
0.30 × 0.25 × 0.25 mm

Data collection

XtaLAB Synergy, Single source at home/near, HyPix3000 diffractometer
Radiation source: fine-focus sealed X-ray tube, Enhance (Cu) X-ray Source
Graphite monochromator
Detector resolution: 10.2576 pixels mm^{-1}
ω scans
Absorption correction: multi-scan (CrysAlis PRO; Rigaku OD, 2020)
T_{min} = 0.906, T_{max} = 1.000
32896 measured reflections
3484 independent reflections
2875 reflections with $I \geq 2u(I)$
R_{int} = 0.050
θ_{max} = 76.0°, θ_{min} = 3.8°
h = −28→28
k = −11→12
l = −12→17

Refinement

Refinement on F^2
Least-squares matrix: full
$R[F^2 > 2\sigma(F^2)]$ = 0.035
$wR(F^2)$ = 0.103
S = 1.05
3484 reflections
246 parameters
0 restraints
28 constraints
H atoms treated by a mixture of independent and constrained refinement
$w = 1/[\sigma^2(F_o^2) + (0.0545P)^2 + 0.3951P]$ where $P = (F_o^2 + 2F_c^2)/3$
$(\Delta/\sigma)_{max}$ = 0.001
$\Delta\rho_{max}$ = 0.23 e Å^{-3}
$\Delta\rho_{min}$ = −0.25 e Å^{-3}

Fractional atomic coordinates and isotropic or equivalent isotropic displacement parameters (Å²)

	x	*y*	*z*	U_{iso}*/U_{eq}
O1A	0.54314 (4)	0.42827 (9)	0.41538 (7)	0.0506 (3)
N1A	0.44426 (5)	0.51032 (10)	0.33566 (8)	0.0410 (3)
H1A	0.46369 (5)	0.42009 (10)	0.34373 (8)	0.0492 (3)*
C2A	0.46844 (5)	0.62938 (11)	0.35331 (8)	0.0347 (3)
N3A	0.43391 (4)	0.72967 (10)	0.33542 (7)	0.0395 (2)
C4A	0.38259 (5)	0.67161 (12)	0.30455 (9)	0.0388 (3)
C5A	0.32989 (6)	0.72712 (14)	0.27686 (10)	0.0512 (3)
H5A	0.32414 (6)	0.83284 (14)	0.27590 (10)	0.0614 (4)*
C6A	0.28500 (6)	0.64385 (15)	0.25056 (11)	0.0544 (4)
H6A	0.24381 (6)	0.68572 (15)	0.22918 (11)	0.0653 (4)*
C7A	0.29165 (6)	0.50760 (16)	0.25101 (12)	0.0568 (4)
H7A	0.25558 (6)	0.44570 (16)	0.23024 (12)	0.0681 (5)*
C8A	0.34374 (6)	0.45002 (14)	0.27762 (11)	0.0553 (4)
H8A	0.34941 (6)	0.34427 (14)	0.27735 (11)	0.0664 (5)*
C9A	0.38835 (5)	0.53409 (13)	0.30468 (9)	0.0400 (3)
N10A	0.52424 (4)	0.64415 (10)	0.38705 (7)	0.0370 (2)
H10A	0.5399 (7)	0.7384 (15)	0.3954 (10)	0.042 (4)*
C11A	0.55827 (5)	0.54332 (12)	0.41863 (9)	0.0375 (3)
C12A	0.61590 (5)	0.58512 (13)	0.45685 (10)	0.0447 (3)
H12A	0.6338 (2)	0.5070 (4)	0.4988 (6)	0.0670 (5)*
H12B	0.64500 (14)	0.6068 (9)	0.39989 (10)	0.0670 (5)*
H12C	0.61036 (8)	0.6717 (6)	0.4994 (6)	0.0670 (5)*
O1B	0.44986 (5)	0.22170 (9)	0.36385 (8)	0.0588 (3)
N1B	0.55554 (5)	0.13757 (10)	0.41569 (8)	0.0421 (3)
H1B	0.53532 (5)	0.22762 (10)	0.41509 (8)	0.0505 (3)*
C2B	0.53160 (5)	0.02000 (12)	0.39257 (8)	0.0364 (3)
N3B	0.56756 (5)	−0.08061 (10)	0.39924 (8)	0.0392 (2)
C4B	0.61967 (5)	−0.02432 (12)	0.42884 (9)	0.0374 (3)
C5B	0.67373 (6)	−0.08151 (13)	0.44646 (10)	0.0466 (3)
H5B	0.68069 (6)	−0.18583 (13)	0.43602 (10)	0.0559 (4)*
C6B	0.71827 (6)	−0.00072 (14)	0.47777 (11)	0.0522 (4)
H6B	0.76041 (6)	−0.04342 (14)	0.49250 (11)	0.0626 (4)*
C7B	0.71020 (6)	0.13435 (15)	0.49078 (11)	0.0543 (4)
H7B	0.74578 (6)	0.19383 (15)	0.51665 (11)	0.0651 (4)*
C8B	0.65723 (6)	0.19316 (14)	0.47100 (11)	0.0518 (3)
H8B	0.65092 (6)	0.29809 (14)	0.47923 (11)	0.0621 (4)*
C9B	0.61259 (5)	0.11201 (12)	0.44021 (9)	0.0398 (3)
N10B	0.47449 (5)	0.00536 (10)	0.36460 (8)	0.0391 (2)
H10B	0.4577 (6)	−0.0867 (14)	0.3530 (9)	0.035 (3)*
C11B	0.43657 (6)	0.10695 (12)	0.35088 (9)	0.0409 (3)
C12B	0.37728 (6)	0.06656 (14)	0.31914 (11)	0.0511 (3)
H12D	0.34675 (10)	0.1440 (5)	0.3343 (7)	0.0767 (5)*
H12E	0.37793 (12)	0.0484 (10)	0.24493 (17)	0.0767 (5)*
H12F	0.3645 (2)	−0.0217 (6)	0.3553 (6)	0.0767 (5)*

Atomic displacement parameters (Å²)

	U^{11}	U^{22}	U^{33}	U^{12}	U^{13}	U^{23}
O1A	0.0473 (5)	0.0266 (5)	0.0779 (7)	−0.0012 (4)	−0.0113 (5)	0.0061 (4)
N1A	0.0401 (6)	0.0268 (5)	0.0562 (6)	−0.0025 (4)	−0.0057 (5)	0.0044 (4)
C2A	0.0353 (6)	0.0264 (6)	0.0425 (6)	−0.0005 (4)	−0.0006 (5)	0.0012 (4)
N3A	0.0348 (5)	0.0287 (5)	0.0550 (6)	0.0016 (4)	−0.0055 (4)	−0.0033 (4)
C4A	0.0335 (6)	0.0346 (7)	0.0483 (6)	0.0001 (5)	−0.0025 (5)	−0.0012 (5)
C5A	0.0385 (7)	0.0416 (8)	0.0734 (9)	0.0036 (6)	−0.0100 (6)	−0.0063 (6)
C6A	0.0346 (7)	0.0553 (9)	0.0733 (9)	−0.0007 (6)	−0.0091 (6)	−0.0003 (7)
C7A	0.0411 (8)	0.0521 (9)	0.0771 (10)	−0.0162 (6)	−0.0132 (7)	0.0086 (7)
C8A	0.0502 (8)	0.0379 (8)	0.0778 (10)	−0.0123 (6)	−0.0158 (7)	0.0113 (7)
C9A	0.0362 (6)	0.0354 (7)	0.0484 (7)	−0.0041 (5)	−0.0036 (5)	0.0054 (5)
N10A	0.0338 (5)	0.0265 (5)	0.0505 (6)	−0.0005 (4)	−0.0030 (4)	0.0018 (4)
C11A	0.0343 (6)	0.0298 (6)	0.0483 (6)	−0.0001 (5)	−0.0015 (5)	0.0032 (5)
C12A	0.0376 (7)	0.0381 (7)	0.0584 (8)	−0.0004 (5)	−0.0061 (5)	0.0033 (6)
O1B	0.0508 (6)	0.0281 (5)	0.0976 (8)	0.0014 (4)	−0.0140 (5)	0.0000 (5)
N1B	0.0411 (6)	0.0272 (5)	0.0579 (6)	0.0005 (4)	−0.0015 (5)	−0.0021 (4)
C2B	0.0390 (6)	0.0270 (6)	0.0433 (6)	0.0005 (5)	−0.0006 (5)	−0.0003 (5)
N3B	0.0374 (5)	0.0275 (5)	0.0527 (6)	0.0006 (4)	−0.0021 (4)	−0.0037 (4)
C4B	0.0352 (6)	0.0315 (6)	0.0456 (6)	−0.0012 (5)	0.0024 (5)	−0.0018 (5)
C5B	0.0369 (7)	0.0370 (7)	0.0659 (8)	0.0011 (5)	0.0006 (6)	−0.0020 (6)
C6B	0.0346 (7)	0.0476 (8)	0.0743 (9)	−0.0032 (6)	0.0015 (6)	−0.0008 (7)
C7B	0.0378 (7)	0.0479 (8)	0.0771 (9)	−0.0102 (6)	0.0006 (7)	−0.0056 (7)
C8B	0.0448 (8)	0.0348 (7)	0.0757 (9)	−0.0068 (6)	−0.0003 (7)	−0.0066 (6)
C9B	0.0386 (6)	0.0319 (6)	0.0489 (7)	−0.0023 (5)	0.0008 (5)	−0.0018 (5)
N10B	0.0378 (5)	0.0288 (5)	0.0509 (6)	0.0007 (4)	−0.0035 (4)	−0.0024 (4)
C11B	0.0403 (7)	0.0297 (6)	0.0527 (7)	0.0020 (5)	−0.0027 (5)	0.0009 (5)
C12B	0.0435 (7)	0.0410 (8)	0.0688 (9)	0.0024 (6)	−0.0086 (6)	−0.0020 (6)

Geometric parameters (Å, º)

O1A—C11A	1.2212 (15)	O1B—C11B	1.2202 (16)
N1A—H1A	1.0270	N1B—H1B	1.0270
N1A—C2A	1.3560 (15)	N1B—C2B	1.3569 (16)
N1A—C9A	1.3818 (16)	N1B—C9B	1.3835 (16)
C2A—N3A	1.3177 (15)	C2B—N3B	1.3190 (15)
C2A—N10A	1.3797 (16)	C2B—N10B	1.3818 (16)
N3A—C4A	1.3920 (15)	N3B—C4B	1.3945 (16)
C4A—C5A	1.3951 (17)	C4B—C5B	1.3960 (17)
C4A—C9A	1.4043 (18)	C4B—C9B	1.4050 (17)
C5A—H5A	1.0830	C5B—H5B	1.0830
C5A—C6A	1.3874 (19)	C5B—C6B	1.3876 (18)
C6A—H6A	1.0830	C6B—H6B	1.0830
C6A—C7A	1.394 (2)	C6B—C7B	1.398 (2)
C7A—H7A	1.0830	C7B—H7B	1.0830
C7A—C8A	1.387 (2)	C7B—C8B	1.387 (2)
C8A—H8A	1.0830	C8B—H8B	1.0830

C8A—C9A	1.3908 (18)	C8B—C9B	1.3890 (18)
N10A—H10A	1.031 (15)	N10B—H10B	1.026 (14)
N10A—C11A	1.3667 (15)	N10B—C11B	1.3661 (16)
C11A—C12A	1.4957 (17)	C11B—C12B	1.4953 (18)
C12A—H12A	1.0770	C12B—H12D	1.0770
C12A—H12B	1.0770	C12B—H12E	1.0770
C12A—H12C	1.0770	C12B—H12F	1.0770

C2A—N1A—H1A	126.71 (7)	C2B—N1B—H1B	126.83 (7)
C9A—N1A—H1A	126.71 (7)	C9B—N1B—H1B	126.83 (7)
C9A—N1A—C2A	106.59 (10)	C9B—N1B—C2B	106.35 (10)
N3A—C2A—N1A	114.03 (11)	N3B—C2B—N1B	114.25 (11)
N10A—C2A—N1A	122.96 (11)	N10B—C2B—N1B	123.47 (11)
N10A—C2A—N3A	123.01 (10)	N10B—C2B—N3B	122.28 (11)
C4A—N3A—C2A	104.17 (10)	C4B—N3B—C2B	104.08 (10)
C5A—C4A—N3A	130.99 (12)	C5B—C4B—N3B	130.55 (12)
C9A—C4A—N3A	109.98 (11)	C9B—C4B—N3B	109.89 (11)
C9A—C4A—C5A	119.02 (12)	C9B—C4B—C5B	119.56 (12)
H5A—C5A—C4A	120.75 (8)	H5B—C5B—C4B	120.99 (8)
C6A—C5A—C4A	118.51 (13)	C6B—C5B—C4B	118.03 (12)
C6A—C5A—H5A	120.75 (9)	C6B—C5B—H5B	120.99 (8)
H6A—C6A—C5A	119.22 (9)	H6B—C6B—C5B	119.13 (8)
C7A—C6A—C5A	121.56 (13)	C7B—C6B—C5B	121.74 (13)
C7A—C6A—H6A	119.22 (8)	C7B—C6B—H6B	119.13 (8)
H7A—C7A—C6A	119.48 (8)	H7B—C7B—C6B	119.56 (8)
C8A—C7A—C6A	121.04 (13)	C8B—C7B—C6B	120.87 (13)
C8A—C7A—H7A	119.48 (9)	C8B—C7B—H7B	119.56 (8)
H8A—C8A—C7A	121.48 (9)	H8B—C8B—C7B	121.36 (8)
C9A—C8A—C7A	117.05 (13)	C9B—C8B—C7B	117.29 (13)
C9A—C8A—H8A	121.48 (8)	C9B—C8B—H8B	121.36 (8)
C4A—C9A—N1A	105.22 (11)	C4B—C9B—N1B	105.43 (11)
C8A—C9A—N1A	131.98 (12)	C8B—C9B—N1B	132.10 (12)
C8A—C9A—C4A	122.81 (12)	C8B—C9B—C4B	122.47 (12)
H10A—N10A—C2A	117.8 (8)	H10B—N10B—C2B	120.3 (8)
C11A—N10A—C2A	124.54 (10)	C11B—N10B—C2B	124.58 (11)
C11A—N10A—H10A	117.3 (8)	C11B—N10B—H10B	115.2 (8)
N10A—C11A—O1A	122.85 (11)	N10B—C11B—O1B	122.75 (12)
C12A—C11A—O1A	122.60 (11)	C12B—C11B—O1B	122.50 (12)
C12A—C11A—N10A	114.55 (11)	C12B—C11B—N10B	114.75 (11)
H12A—C12A—C11A	109.5	H12D—C12B—C11B	109.5
H12B—C12A—C11A	109.5	H12E—C12B—C11B	109.5
H12B—C12A—H12A	109.5	H12E—C12B—H12D	109.5
H12C—C12A—C11A	109.5	H12F—C12B—C11B	109.5
H12C—C12A—H12A	109.5	H12F—C12B—H12D	109.5
H12C—C12A—H12B	109.5	H12F—C12B—H12E	109.5

O1A—C11A—N10A—C2A	3.85 (16)	O1B—C11B—N10B—C2B	−1.22 (17)
N1A—C2A—N3A—C4A	0.75 (11)	N1B—C2B—N3B—C4B	−0.30 (12)

N1A—C2A—N10A—C11A	−9.55 (15)	N1B—C2B—N10B—C11B	4.53 (15)
N1A—C9A—C4A—N3A	−0.37 (11)	N1B—C9B—C4B—N3B	−0.84 (11)
N1A—C9A—C4A—C5A	−179.52 (10)	N1B—C9B—C4B—C5B	178.69 (10)
N1A—C9A—C8A—C7A	179.10 (17)	N1B—C9B—C8B—C7B	179.35 (17)
C2A—N1A—C9A—C4A	0.79 (11)	C2B—N1B—C9B—C4B	0.63 (11)
C2A—N1A—C9A—C8A	−179.21 (12)	C2B—N1B—C9B—C8B	−178.87 (11)
C2A—N3A—C4A—C5A	178.81 (11)	C2B—N3B—C4B—C5B	−178.77 (10)
C2A—N3A—C4A—C9A	−0.21 (11)	C2B—N3B—C4B—C9B	0.70 (11)
C2A—N10A—C11A—C12A	−176.65 (13)	C2B—N10B—C11B—C12B	179.08 (14)
N3A—C2A—N1A—C9A	−1.01 (12)	N3B—C2B—N1B—C9B	−0.22 (12)
N3A—C2A—N10A—C11A	170.41 (12)	N3B—C2B—N10B—C11B	−175.67 (12)
N3A—C4A—C5A—C6A	−178.83 (16)	N3B—C4B—C5B—C6B	−178.53 (15)
N3A—C4A—C9A—C8A	179.63 (11)	N3B—C4B—C9B—C8B	178.72 (11)
C4A—N3A—C2A—N10A	−179.22 (9)	C4B—N3B—C2B—N10B	179.88 (9)
C4A—C5A—C6A—C7A	−0.24 (17)	C4B—C5B—C6B—C7B	−0.62 (16)
C4A—C9A—C8A—C7A	−0.90 (16)	C4B—C9B—C8B—C7B	−0.09 (15)
C5A—C4A—C9A—C8A	0.48 (16)	C5B—C4B—C9B—C8B	−1.74 (16)
C5A—C6A—C7A—C8A	−0.20 (19)	C5B—C6B—C7B—C8B	−1.23 (19)
C6A—C5A—C4A—C9A	0.11 (17)	C6B—C5B—C4B—C9B	2.04 (16)
C6A—C7A—C8A—C9A	0.75 (19)	C6B—C7B—C8B—C9B	1.55 (18)
C9A—N1A—C2A—N10A	178.96 (9)	C9B—N1B—C2B—N10B	179.60 (10)

Hydrogen-bond geometry (Å, º)

D—H···*A*	*D*—H	H···*A*	*D*···*A*	*D*—H···*A*
N1*A*—H1*A*···O1*B*	1.03 (1)	2.06 (1)	2.9647 (15)	145 (1)
N1*B*—H1*B*···O1*A*	1.03 (1)	2.05 (1)	2.9693 (15)	148 (1)
N1*A*—H1*A*···O1*A*	1.03 (1)	2.10 (1)	2.6780 (16)	114 (1)
N1*B*—H1*B*···O1*B*	1.03 (1)	2.10 (1)	2.6822 (17)	114 (1)
N10*A*—H10*A*···N3*B*^{i}	1.031 (15)	1.948 (15)	2.9757 (16)	174.7 (13)
N10*B*—H10*B*···N3*A*^{ii}	1.026 (14)	1.962 (14)	2.9837 (16)	173.7 (11)

Symmetry codes: (i) *x*, *y*+1, *z*; (ii) *x*, *y*−1, *z*.